

# Stable noise-like pulse generation in all-PM mode-locked Tm-doped fiber laser based on NOLM

Meng Wang (王蒙)<sup>1,2</sup>, Minqiu Liu (刘敏秋)<sup>1</sup>, Yewang Chen (陈业旺)<sup>1</sup>, Deqin Ouyang (欧阳德钦)<sup>1</sup>, Junqing Zhao (赵俊清)<sup>1</sup>, Jihong Pei (裴继红)<sup>2</sup>, and Shuangchen Ruan (阮双琛)<sup>1\*</sup>

<sup>1</sup>Key Laboratory of Advanced Optical Precision Manufacturing Technology of Guangdong Higher Education Institutes, Sino-German College of Intelligent Manufacturing, Shenzhen Technology University, Shenzhen 518118, China

<sup>2</sup>College of Electronics and Information Engineering, Shenzhen University, Shenzhen 518060, China

\*Corresponding author: [scruan@sztu.edu.cn](mailto:scruan@sztu.edu.cn)

Received December 24, 2020 | Accepted March 4, 2021 | Posted Online June 18, 2021

A stable noise-like (NL) mode-locked Tm-doped fiber laser (TDFL) relying on a nonlinear optical loop mirror (NOLM) was experimentally presented. Different from the previous NL mode-locked TDFL with NOLM, the entire polarization-maintaining (PM) fiber construction was utilized in our laser cavity, which makes the oscillator have a better resistance to environmental perturbations. The robust TDFL can deliver stable bound-state NL pulses with a pulse envelope tunable from  $\sim 14.1$  ns to  $\sim 23.6$  ns and maximum pulse energy of  $\sim 40.3$  nJ at a repetition rate of  $\sim 980.6$  kHz. Meanwhile, the all-PM fiber laser shows good power stability (less than  $\sim 0.7\%$ ) and repeatability.

**Keywords:** noise-like pulse; all-polarization-maintaining fiber; nonlinear loop mirror; Tm-doped fiber laser.

**DOI:** [10.3788/COL202119.091402](https://doi.org/10.3788/COL202119.091402)

## 1. Introduction

A pulse fiber laser operating at the  $2\ \mu\text{m}$  spectrum region with its extensive applications in industry processing, medical treatment, and scientific research has been widely studied in recent years. Among the techniques for pulse laser generation, passive mode-locking is an effective and convenient one. Based on the different dynamics of mode-locking and cavity conditions, different kinds of mode-locked pulses such as conventional soliton<sup>[1]</sup>, dissipative soliton<sup>[2]</sup>, bound-state soliton<sup>[3]</sup>, dissipative soliton resonance<sup>[4,5]</sup>, stretched pulse<sup>[6,7]</sup>, and noise-like (NL) pulse<sup>[8]</sup> were obtained in passively mode-locked Tm-doped fiber lasers (TDFLs).

For the NL pulse, the pulse exhibits a relatively wide envelope ( $\sim$ nanoseconds or  $\sim$ picoseconds), which contains a bunch of random pulses with different widths and peak intensities. With the help of the autocorrelator, the ultrashort coherent spike can be observed in the autocorrelation trace<sup>[9]</sup>. Owing to the special pulse structure, the NL pulse can be directly obtained from an oscillator with a high pulse energy [ $\sim$ nanojoule (nJ) level] and relatively low peak power, which makes it useful in many applications such as supercontinuum generation and industrial processing<sup>[10–12]</sup>. Till now, many NL mode-locked fiber lasers in the  $2\ \mu\text{m}$  spectrum regime were reported relying on different mode-locking techniques, such as nonlinear polarization rotation (NPR), nonlinear optical loop mirror (NOLM), nonlinear amplifying loop mirror (NALM), and

material-based saturable absorber (SA). Relying on the NPR technique, Sobon *et al.* reported an NL mode-locked TDFL in an all-normal dispersion cavity with the maximum pulse energy of  $\sim 1.3$  nJ<sup>[13]</sup>. In the anomalous dispersion condition, He *et al.* and Liu *et al.* also studied NL mode-locking in TDFLs with pulse energies of  $\sim 17.3$  nJ and  $\sim 12.3$  nJ, respectively<sup>[14,15]</sup>. As for the nonlinear loop mirror method, Li *et al.* reported an NL mode-locked pulse with the highest pulse energy of  $\sim 249$  nJ, and Wang *et al.* achieved an NL pulse with pulse energy of  $\sim 97.4$  nJ<sup>[16,17]</sup>. Moreover, based on the material-based SA, the NL pulse in the TDFL also was reported. In the graphene-based NL mode-locked TDFL, the maximum pulse energy of  $\sim 51.5$  nJ was achieved after amplification<sup>[8]</sup>. By utilizing the carbon nanotube as an SA, the NL pulse with pulse energy of  $\sim 1.27$  nJ was obtained<sup>[18]</sup>. Nevertheless, we note that the previous studies were based on the standard single mode fiber, which is sensitive to the environmental disturbance, such as temperature or fiber vibration. Meanwhile, the polarization controller is always an essential component for initializing mode-locking, which seriously weakens the repeatability of the fiber laser and limits the usage in laboratories.

To solve the issue of environmental sensitivity, the all-polarization-maintaining (PM) fiber configuration is a potential and available solution, since it is immune to the slight fluctuation of the polarization state. In the recent years, some works about passively mode-locked TDFLs with an all-PM fiber configuration were reported. By using the semiconductor saturable absorption

mirror (SESAM) as an SA, Liu *et al.* achieved mode-locked pulses with a pulse duration of  $\sim 10$  ps<sup>[19]</sup>. Based on the graphene SA, soliton and stretched pulses were separately obtained by Sobon and the co-authors<sup>[20,21]</sup>. In fact, except for the material-based SA, the “artificial” SA (NPR, NALM, and NOLM) also can be used for mode-locking operation in an all-PM fiber configuration, which has been widely studied in the  $\sim 1.1$   $\mu\text{m}$  spectral regime<sup>[22–28]</sup>. In the 2  $\mu\text{m}$  region, Michalska and Swiderski reported a soliton mode-locked TDFL with an all-PM fiber configuration based on NOLM, in which the pulse energy is  $\sim 71$  pJ<sup>[29]</sup>. Moreover, NL pulses were obtained based on NALM<sup>[30]</sup>. The mode-locking mechanism of a nonlinear loop mirror in an all-PM fiber configuration is the same as that in a standard single mode fiber, in which the intensity-dependent transmission was implemented by the interference between two counter-propagating pulses at the coupler, and the phase difference between the two counter-propagating pulses can be easily controlled by adjusting the splitting ratio of the coupler and the length of fibers<sup>[31,32]</sup>. Compared to the material-based SA, such an “artificial” SA has latent advantages of high damage threshold and long work life.

In this paper, we have firstly, to the best of our knowledge, presented an NL mode-locked TDFL based on NOLM with an all-PM fiber configuration. The laser was operated in bound-state NL mode-locking. Meanwhile, owing to the all-PM fiber structure, the laser has a good power stability (less than  $\sim 0.7\%$ ) and repeatability.

## 2. Experimental Setup and Results

The schematic diagram of the all-PM TDFL is depicted in Fig. 1. The gain fiber is a section of  $\sim 3$  m PM Tm-doped fiber (PM-TSF 9/125, Nufern), which was pumped by a  $\sim 1550$  nm fiber laser via a PM fused-taper wavelength division multiplexer (WDM). A polarization-sensitive isolator (ISO) with the fast axis blocked was utilized for ensuring the unidirectional and linear

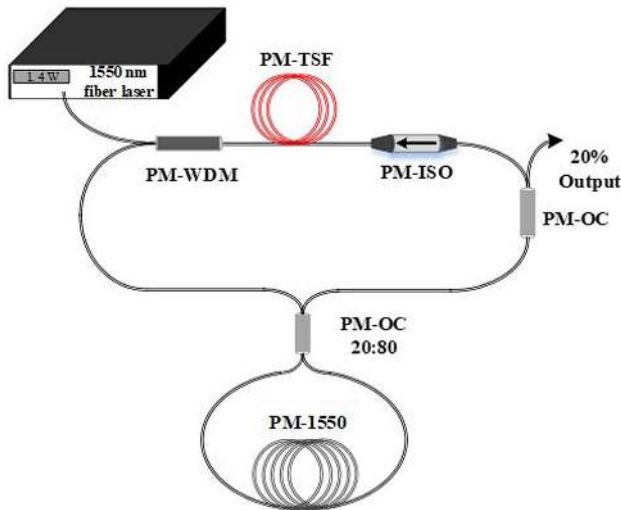


Fig. 1. Schematic diagram of the all-PM Tm-doped fiber laser.

polarization operation. The NOLM was constructed by a  $2 \times 2$  output coupler (OC) with splitting ratio of 20:80 and a piece of  $\sim 196$  m PM fiber (PM-1550XP, Nufern), which provides the intensity-dependent loss in the oscillator. The output laser was extracted by another  $2 \times 1$  coupler with an output ratio of  $\sim 20\%$ . All of the fibers in the cavity are single mode PM fibers (Panda style), which were spliced by a PM fiber fusion splicer (FSM-100 P+, Fujikura) with angle mismatching of less than  $\sim 1^\circ$ . Thus, an “8” shape cavity was constructed with total length of  $\sim 211$  m and net dispersion of  $\sim -14.4$  ps<sup>2</sup>.

The performances of the mode-locked pulse were recorded by an optical spectrum analyzer (AQ6375, Yokogawa), an oscilloscope with 4 GHz bandwidth and 40 GS/s sampling rate (WaveRunner 9000, Teledyne Lecroy), a 12.5 GHz photodetector (ET-5000 F, EOT), an autocorrelator (Pulsecheck 600, APE), and a 26.5 GHz radio frequency (RF) spectrum analyzer (N9020B, Keysight).

With increasing pump power, stable mode-locking operation can self-start at an incident pump power of  $\sim 848$  mW. The high threshold may be caused by the long passive fibers, since the silica single mode fiber has a relatively high transmission loss at 2  $\mu\text{m}$ . Nevertheless, when we utilized a shorter passive fiber (e.g.,  $\sim 100$  m), the threshold of the mode-locking operation was further increased. The reason was mainly considered because of less nonlinear phase accumulation with a shorter passive fiber in the NOLM, since the nonlinear phase is proportional to the length of the loop mirror and peak power, which is inversely proportional to the wavelength<sup>[33]</sup>. Thus, a long piece of passive fiber was used in our oscillator. When the laser operates in stable mode-locked state, it can be maintained with further increasing the pump power. Figure 2 exhibits the evolutions of the spectrum and pulse envelope with pump power. As the pump power increases from  $\sim 848$  mW to  $\sim 1414$  mW, there

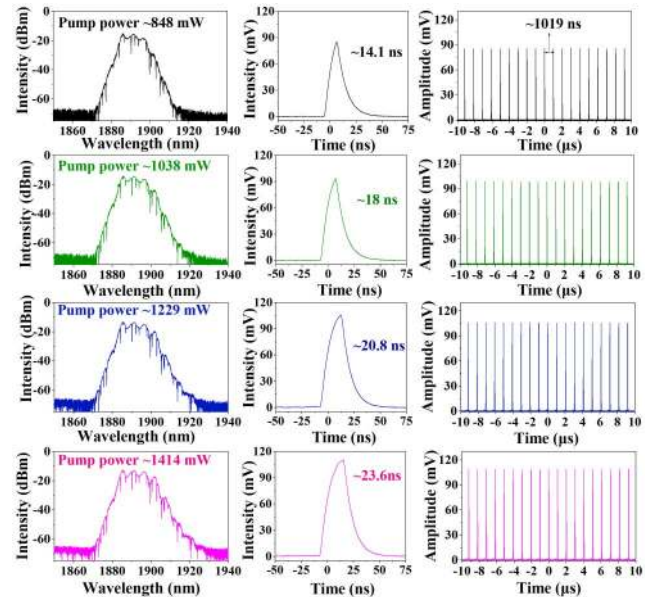


Fig. 2. Evolutions of mode-locked spectrum and pulse envelope, recorded at different incident pump powers.

are no obvious variations in spectral shape and central wavelength ( $\sim 1891$  nm). But, the 3 dB bandwidth of the spectrum was broadened from  $\sim 8$  nm to  $\sim 13$  nm. A similar tendency was also observed in the pulse envelope, which was broadened from  $\sim 14.1$  ns to  $\sim 23.6$  ns. The pulse interval of  $\sim 1019$  ns corresponds to the round-trip time, which is determined by the cavity length of  $\sim 211$  m. To avoid the damage of the components such as WDM and ISO, the maximum incident pump power was limited at  $\sim 1414$  mW.

To further clarify the mode-locking property, the autocorrelation trace was measured at pump power of  $\sim 1414$  mW, as shown in Fig. 3. Three coherent spikes with a time interval of  $\sim 2.2$  ps were measured, which implies the bound-state NL mode-locking of the fiber laser. However, with the limitation of resolution of the autocorrelator (the number of sampling points was fixed at 256), the trace was measured in time span of  $\sim 4.3$  ps, and the three peaks were recorded by adjusting the central position, as exhibited in Figs. 3(a) and 3(b). Meanwhile, a slight modulation of the optical spectrum also can be observed, as shown in Fig. 3(c). The period of the modulation was  $\sim 5.5$  nm ( $\Delta\nu \sim 461$  GHz), which agrees well with the time interval ( $\sim 2.2$  ps) of the coherent spikes according to the relationship of  $\Delta\nu = 1/\tau$ <sup>[3,34]</sup>. The dips in the spectrum mainly result from the strong water absorption lines around the  $1.9 \mu\text{m}$  spectral region<sup>[1]</sup>. Moreover, the full width at half-maximum (FWHM) of the main coherent spike is  $\sim 721$  fs with the Gaussian fitting, as given in Fig. 3(d).

The RF spectrum of the NL pulse was also measured at pump power of  $\sim 1414$  mW, as depicted in Fig. 4. The repetition frequency of  $\sim 980.6$  kHz corresponds to the cavity length of  $\sim 211$  m, which indicates fundamental mode-locking. The signal to noise ratio (SNR) of  $\sim 66$  dB was comparable to that of the previous reported NL mode-locking at the  $2 \mu\text{m}$  regime, which means low amplitude noise of the sub-pulses in the pulse envelope<sup>[14,16]</sup>. Figure 4(b) shows the RF spectrum in a wide span of  $\sim 300$  MHz. A large modulation frequency of

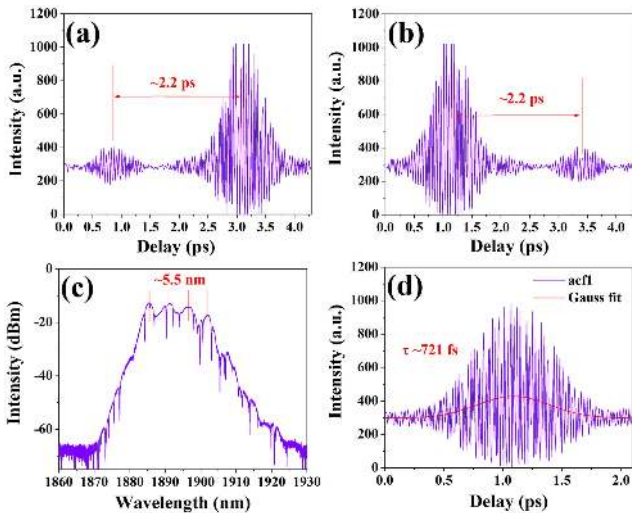


Fig. 3. (a) (b) Autocorrelation traces with time span of 4.3 ps, (c) optical spectrum, and (d) autocorrelation trace with time span of 2.1 ps.

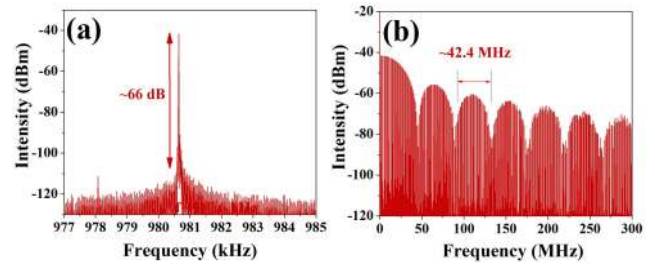


Fig. 4. RF spectra at different spans: (a) 8 MHz; (b) 300 MHz.

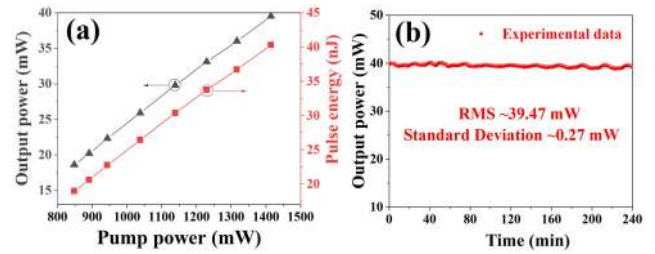


Fig. 5. (a) Evolutions of output power and pulse energy; (b) average output power in 4 h.

$\sim 42.4$  MHz was observed, which satisfies the reciprocal relation of the duration of the NL pulse envelope ( $f_m = \frac{1}{\tau}$ )<sup>[35]</sup>. Thus, the recorded duration of the pulse envelope of  $\sim 23.6$  ns is exact.

Moreover, the performance of output power was measured, as plotted in Fig. 5. The average output power was almost linearly increased from  $\sim 18.6$  mW to  $\sim 39.5$  mW as the pump power was enhanced from  $\sim 848$  mW to  $\sim 1414$  mW. After dividing the average power by repetition frequency, the pulse energy with maximum value of  $\sim 40.3$  nJ was calculated, as plotted in Fig. 5(a). At the pump power of  $\sim 1414$  mW, the stability of the output power was monitored in 4 h with time intervals of 10 s, as illustrated in Fig. 5(b). The root mean square (RMS) value of the average output power was calculated to be  $\sim 39.47$  mW with a standard deviation of  $\sim 0.27$  mW, which indicates good stability of the output power with fluctuation of  $\sim 0.7\%$ . To check the repeatability of the fiber laser, we restarted the fiber laser and measured the average output power at the fixed pump power of  $\sim 1414$  mW in the following three days. As shown in Figs. 6(a)–6(c), the TDFL still operated at a stable NL mode-locked state with stable output power of  $\sim 39$  mW. Meanwhile, the fiber laser shows a good resistance to vibration. During the experiment, by flapping the platform and directly

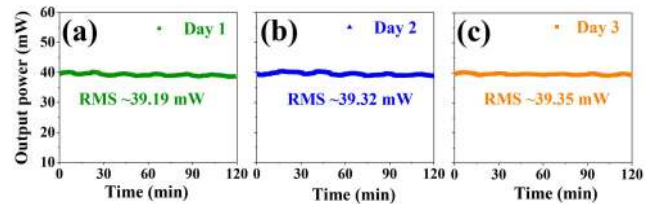


Fig. 6. Performances of output power in three days.

juggling the long passive fiber, the NL mode-locking operation can be well maintained without any notable variations.

### 3. Conclusion

In this paper, a stable bound-state NL mode-locked all-PM TDFL based on NOLM was experimentally demonstrated. The NL pulse has the maximum pulse energy of  $\sim 40.3$  nJ, and the width of the pulse envelope can be tuned from  $\sim 14.1$  ns to  $\sim 23.6$  ns. The pulse energy might be further increased by a larger pump power with high power fiber components. In addition, the fiber laser exhibited good power stability with power fluctuation less than  $\sim 0.7\%$  during 4 h monitoring. Meanwhile, owing to the all-PM fiber configuration without a polarization controller, the mode-locked fiber laser has good repeatability. This pulse laser source has potential applications in polymer processing and supercontinuum generation after further amplification.

### Acknowledgement

This work was supported by the National Natural Science Foundation of China (NSFC) (No. 61905146), the China Postdoctoral Science Foundation (No. 2020M682864), and the Shenzhen Key Project for Technology Development (Nos. JSGG20190819175801678 and JSGG20191129105838333).

### References

- J. Sotor, G. Sobon, M. Kowalczyk, W. Macherzynski, P. Paletko, and K. M. Abramski, "Ultrafast thulium-doped fiber laser mode locked with black phosphorus," *Opt. Lett.* **40**, 3885 (2015).
- C. Huang, C. Wang, W. Shang, N. Yang, Y. Tang, and J. Xu, "Developing high energy dissipative soliton fiber lasers at 2 micron," *Sci. Rep.* **5**, 13680 (2015).
- M. Chernysheva, A. Bednyakova, M. A. Araimi, R. C. T. Howe, G. Hu, T. Hasan, A. Gambetta, G. Galzerano, M. Rummeli, and A. Rozhin, "Double-wall carbon nanotube hybrid mode-locker in Tm-doped fibre laser: a novel mechanism for robust bound-state solitons generation," *Sci. Rep.* **7**, 44314 (2017).
- J. Zhao, D. Ouyang, Z. Zheng, M. Liu, X. Ren, C. Li, S. Ruan, and W. Xie, "100 W dissipative soliton resonances from a thulium-doped double-clad all-fiber-format MOPA system," *Opt. Express* **24**, 12072 (2016).
- H. Wang, T. Du, Y. Li, J. Zou, K. Wang, F. Zheng, J. Fu, J. Yang, H. Fu, and Z. Luo, "2080 nm long-wavelength, high-power dissipative soliton resonance in a dumbbell-shaped thulium-doped fiber laser," *Chin. Opt. Lett.* **17**, 030602 (2019).
- F. Haxsen, A. Ruehl, M. Engelbrecht, D. Wandt, U. Morgner, and D. Kracht, "Stretched-pulse operation of a thulium-doped fiber laser," *Opt. Express* **16**, 20471 (2008).
- Y. Wang, S. Alam, E. D. Obraztsova, A. S. Pozharov, S. Y. Set, and S. Yamashita, "Generation of stretched pulses and dissipative solitons at 2  $\mu\text{m}$  from an all-fiber mode-locked laser using carbon nanotube saturable absorbers," *Opt. Lett.* **41**, 3864 (2016).
- G. Sobon, J. Sotor, A. Przewolka, I. Pasternak, W. Strupinski, and K. Abramski, "Amplification of noise-like pulses generated from a graphene-based Tm-doped all-fiber laser," *Opt. Express* **24**, 20359 (2016).
- Z. Zhang, J. Tian, C. Xu, R. Xu, Y. Cui, B. Zhuang, and Y. Song, "Noise-like pulse with a 690 fs pedestal generated from a nonlinear Yb-doped fiber amplification system," *Chin. Opt. Lett.* **18**, 121403 (2020).
- S. S. Lin, S. K. Hwang, and J. M. Liu, "Supercontinuum generation in highly nonlinear fibers using amplified noise-like optical pulses," *Opt. Express* **22**, 4152 (2014).
- E. Hernández-Escobar, M. Bello-Jiménez, O. Pottiez, B. Ibarra-Escamilla, and M. V. Andrés, "Flat supercontinuum generation pumped by amplified noise-like pulses from a figure-eight erbium-doped fiber laser," *Laser Phys. Lett.* **14**, 105104 (2017).
- M. Malinauskas, A. Žukauskas, S. Hasegawa, Y. Hayasaki, V. Mizeikis, R. Buividas, and Juodkasis Saulius, "Ultrafast laser processing of materials: from science to industry," *Light: Sci. Appl.* **5**, e16133 (2016).
- G. Sobon, J. Sotor, T. Martynkien, and K. M. Abramski, "Ultra-broadband dissipative soliton and noise-like pulse generation from a normal dispersion mode-locked Tm-doped all-fiber laser," *Opt. Express* **24**, 6156 (2016).
- X. He, A. Luo, Q. Yang, T. Yang, X. Yuan, S. Xu, Q. Qian, D. Chen, Z. Luo, W. Xu, and Z. Yang, "60 nm bandwidth, 17 nJ noise-like pulse generation from a thulium-doped fiber ring laser," *Appl. Phys. Express* **6**, 112702 (2013).
- S. Liu, F. Yan, Y. Li, L. Zhang, Z. Bai, H. Zhou, and Y. Hou, "Noise-like pulse generation from a thulium-doped fiber laser using nonlinear polarization rotation with different net anomalous dispersion," *Photon. Res.* **4**, 318 (2016).
- J. Li, Z. Zhang, Z. Sun, H. Luo, Y. Liu, Z. Yan, C. Mou, L. Zhang, and S. K. Turitsyn, "All-fiber passively mode-locked Tm-doped NOLM-based oscillator operating at 2- $\mu\text{m}$  in both soliton and noisy-pulse regimes," *Opt. Express* **22**, 7875 (2014).
- X. Wang, Q. Xia, and B. Gu, "A 1.9  $\mu\text{m}$  noise-like mode-locked fiber laser based on compact figure-9 resonator," *Opt. Commun.* **434**, 180 (2019).
- Q. Wang, T. Chen, M. Li, B. Zhang, Y. Lu, and K. P. Chen, "All-fiber ultrafast thulium-doped fiber ring laser with dissipative soliton and noise-like output in normal dispersion by single-wall carbon nanotubes," *Appl. Phys. Lett.* **103**, 011103 (2013).
- J. Liu, C. Liu, H. Shi, and P. Wang, "High-power linearly-polarized picosecond thulium-doped all-fiber master-oscillator power-amplifier," *Opt. Express* **24**, 15005 (2016).
- G. Sobon, J. Sotor, I. Pasternak, A. Krajewska, W. Strupinski, and K. M. Abramski, "All-polarization maintaining, graphene-based femtosecond Tm-doped all-fiber laser," *Opt. Express* **23**, 9339 (2015).
- J. Sotor, J. Bogusławski, T. Martynkien, P. Mergo, A. Krajewska, A. Przewłoka, W. Strupinski, and G. Sobon, "All-polarization-maintaining, stretched-pulse Tm-doped fiber laser, mode-locked by a graphene saturable absorber," *Opt. Lett.* **42**, 1592 (2017).
- X. Shen, W. Li, and H. Zeng, "Polarized dissipative solitons in all-polarization-maintained fiber laser with long-term stable self-started mode-locking," *Appl. Phys. Lett.* **105**, 101109 (2014).
- Y. Wang, L. Zhang, Z. Zhuo, and S. Guo, "Cross-splicing method for compensating fiber birefringence in polarization-maintaining fiber ring laser mode locked by nonlinear polarization evolution," *Appl. Opt.* **55**, 5766 (2016).
- J. Szczepanek, T. M. Kardas, C. Radzewicz, and Y. Stepanenko, "Ultrafast laser mode-locked using nonlinear polarization evolution in polarization maintaining fibers," *Opt. Lett.* **42**, 575 (2017).
- J. Szczepanek, T. M. Kardas, C. Radzewicz, and Y. Stepanenko, "Nonlinear polarization evolution of ultrashort pulses in polarization maintaining fibers," *Opt. Express* **26**, 13590 (2018).
- Z. Wu, Q. Wei, P. Huang, S. Fu, D. Liu, and T. Huang, "Nonlinear polarization evolution mode-locked YDFL based on all-PM fiber cavity," *IEEE Photon. J.* **12**, 1501807 (2020).
- C. Agueraray, N. G. Broderick, M. Erkintalo, J. S. Chen, and V. Kruglov, "Mode-locked femtosecond all-normal all-PM Yb-doped fiber laser using a nonlinear amplifying loop mirror," *Opt. Express* **20**, 10545 (2012).
- A. A. Borodkin, D. V. Khudyakov, and S. K. Vartapetov, "Subnanosecond and picosecond generation regimes of all-PM Yb-doped fiber laser mode-locked by NOLM," *J. Phys. Conf. Ser.* **747**, 012053 (2016).
- M. Michalska and J. Swiderski, "All-fiber thulium-doped mode-locked fiber laser and amplifier based on nonlinear fiber loop mirror," *Opt. Laser Technol.* **118**, 121 (2019).

30. M. Michalska and J. Swiderski, "Noise-like pulse generation using polarization maintaining mode-locked thulium-doped fiber laser with nonlinear amplifying loop mirror," *IEEE Photon. J.* **11**, 1504710 (2019).
31. J. Szczepanek, T. M. Kardas, M. Michalska, C. Radzewicz, and Y. Stepanenko, "Simple all-PM-fiber laser mode-locked with a nonlinear loop mirror," *Opt. Lett.* **40**, 3500 (2015).
32. M. Wang, Y. J. Huang, J. W. Yang, Y. Zhang, and S. C. Ruan, "Multi-wavelength mode-locked thulium-doped fiber laser based on a fiber-optic Fabry-Perot interferometer and a nonlinear optical loop mirror," *Laser Phys. Lett.* **15**, 085110 (2018).
33. N. J. Doran and D. Wood, "Nonlinear-optical loop mirror," *Opt. Lett.* **13**, 56 (1988).
34. R. Lü, Y. Wang, J. Wang, W. Ren, L. Li, S. Liu, Z. Chen, Y. Li, H. Wang, and F. Fu, "Soliton and bound-state soliton mode-locked fiber laser based on a MoS<sub>2</sub>/fluorine mica Langmuir-Blodgett film saturable absorber," *Photon. Res.* **7**, 431 (2019).
35. X. Li, X. Liu, X. Hu, L. Wang, H. Lu, Y. Wang, and W. Zhao, "Long-cavity passively mode-locked fiber ring laser with high-energy rectangular-shape pulses in anomalous dispersion regime," *Opt. Lett.* **35**, 19 (2010).